Inorg. Chem. **2000,** *39,* 3181−3191 **3181**

Water Adsorption and Hydrolysis on Molecular Transition Metal Oxides and Oxyhydroxides

J. R. Tobias Johnson*

Inorganic Chemistry, Department of Chemistry, Göteborg University, S-412 96 Göteborg, Sweden

Itai Panas

Department of Inorganic Environmental Chemistry, Chalmers University of Technology,
S-412 96 Göteborg, Sweden

Received September 27, 1999

Addition of water to molecular transition metal oxides (TiO_2(g) and CrO_3(g)) and oxyhydroxides (ScO(OH)(g), VO_2(OH)(g), and MnO_3(OH)(g)) was studied by means of quantum chemistry. In the investigated reactions, each reaction step comprised the breaking of one M═O bond and the formation of two OH groups. Exothermicity was observed when the product had tetrahedral or lower oxygen coordination. The reactions were found to involve stable water complexes as intermediates. The stabilities of such complexes were accentuated in the addition reaction $Sc(OH)_3$(g) + H_2O(g), in which the formation of a tetrahedral complex was found exothermic. For $VO(OH)_3$(g), $CrO_2(OH)_2$(g), and MnO_3(OH)(g), water addition to the remaining M═O bonds was found endothermic, whereas the formation of water complexes, using hydrogen bonds and preserving the oxyhydroxide kernel, was preferred. Thus, the sequence of such kernels for water clustering in the investigated reactions was found to be $Sc(OH)_3$·H_2O(g), $Ti(OH)_4$(g), $VO(OH)_3$(g), $CrO_2(OH)_2$(g), and MnO_3(OH)(g). These stability considerations are important, as $CrO_2(OH)_2$(g) is believed to be the product of water-induced degradation of the protective chromium oxide scale on stainless steel at elevated temperatures.

1. Introduction

Titanium and chromium oxides are generally seen as chemically stable materials that make up protective oxide films on Ti and Cr metals. These films are understood to grow by oxygen diffusion and conduction of electrons and metal ions across the oxide layer, as modeled first by Wagner.[1,2] The rate of oxidation depends critically on the conduction properties and thickness of the oxide film. At equilibrium, the oxygen/metal ratio decreases gradually upon approaching the metal substrate. Active corrosion implies removal of surface oxide material and thus exposing the metal to further oxidation. Evaporation of molecular oxides comprises one such process, which was first described by Tedmon.[3] Such destructive fragmentation into molecular species includes gas phase products formed in any chemically aggressive environment.

Recently, the water-induced degradation of the protective chromium oxide scale on stainless steel was investigated by means of experiment[4] and a mechanistic study was performed by means of theory.[5] It was suggested[4] that Cr leaves the substrate as $CrO_2(OH)_2$(g), and the enthalpy for the formation of this product was estimated.[5] The result was put in context by considering similar reactions for the whole transition metal sequence Sc−Mn. As water is known to be a corrosive agent on materials protected by such surface oxides, it becomes interesting to investigate a variety of possible reactions with water. While the direct action of water on a particular oxide site at the surface has been modeled,[5] the present work focuses on secondary reactions with water. Particularly, the stability of $CrO_2(OH)_2$(g) toward emitting water is addressed and put in context with the stabilities of other $MO_x(OH)_y$(g) species. Hence, water addition to TiO_2(g) and CrO_3(g) is investigated, and compared within the transition metal sequence Sc−Mn to the oxyhydroxides ScO(OH)(g), VO_2(OH)(g), and MnO_3(OH)(g). Transition state structures and stabilities are also estimated for these reactions. Reactants and reaction products for the following reactions are investigated by means of quantum chemistry:

$$\begin{gathered}\mathrm{ScO(OH)(g) + H_2O(g) \rightarrow ScO(OH){\cdot}H_2O(g)}\\ \mathrm{ScO(OH){\cdot}H_2O(g) \rightarrow Sc(OH)_3(g)}\\ \mathrm{Sc(OH)_3(g) + H_2O(g) \rightarrow Sc(OH)_3{\cdot}H_2O(g)}\end{gathered} \tag{R1}$$

$$\begin{gathered}\mathrm{TiO_2(g) + H_2O(g) \rightarrow TiO_2{\cdot}H_2O(g)}\\ \mathrm{TiO_2{\cdot}H_2O(g) \rightarrow TiO(OH)_2(g)}\\ \mathrm{TiO_2{\cdot}H_2O(g) + H_2O(g) \rightarrow TiO_2{\cdot}(H_2O)_2(g)}\\ \mathrm{TiO(OH)_2(g) + H_2O(g) \rightarrow TiO(OH)_2{\cdot}H_2O(g)}\\ \mathrm{TiO_2{\cdot}(H_2O)_2(g) \rightarrow TiO(OH)_2{\cdot}H_2O(g)}\\ \mathrm{TiO(OH)_2{\cdot}H_2O(g) \rightarrow Ti(OH)_4(g)}\end{gathered} \tag{R2}$$

---

(1) Wagner, C. *Z. Phys. Chem. B* **1933**, *21*, 25.
(2) Wagner, C. *Prog. Solid State Chem.* **1975**, *10*, 3.
(3) Tedmon, J. S. *J. Electrochem. Soc.* **1966**, *113*, 766.
(4) Asteman, H.; Svensson, J.-E.; Johansson, L.-G.; Norell, M. *Oxid. Met.* **1999**, *52*, 161.
(5) Johnson, J. R. T.; Panas, I. *Inorg. Chem.* **2000**, *39*, 3192.

10.1021/ic991150h CCC: $19.00

$$\begin{array}{c} VO_2(OH)(g) + H_2O(g) \rightarrow VO_2(OH){\cdot}H_2O(g) \\ VO_2(OH){\cdot}H_2O(g) \rightarrow VO(OH)_3(g) \\ VO(OH)_3(g) + H_2O(g) \rightarrow VO(OH)_3{\cdot}H_2O(g) \\ VO(OH)_3{\cdot}H_2O(g) \rightarrow V(OH)_5(g) \end{array} \qquad (R3)$$

$$\begin{array}{c} CrO_3(g) + H_2O(g) \rightarrow CrO_3{\cdot}H_2O(g) \\ CrO_3{\cdot}H_2O(g) \rightarrow CrO_2(OH)_2(g) \\ CrO_2(OH)_2(g) + H_2O(g) \rightarrow CrO_2(OH)_2{\cdot}H_2O(g) \\ CrO_2(OH)_2{\cdot}H_2O(g) \rightarrow CrO(OH)_4(g) \\ CrO(OH)_4(g) + H_2O(g) \rightarrow CrO(OH)_4{\cdot}H_2O(g) \\ CrO(OH)_4{\cdot}H_2O(g) \rightarrow Cr(OH)_6(g) \end{array} \qquad (R4)$$

$$\begin{array}{c} MnO_3(OH)(g) + H_2O(g) \rightarrow MnO_3(OH){\cdot}H_2O(g) \\ MnO_3(OH){\cdot}H_2O(g) \rightarrow MnO_2(OH)_3(g) \\ (MnO_3(OH)(g) + H_2O(g) \rightarrow MnO(OH)_5(g)) \\ (MnO(OH)_5(g) + H_2O(g) \rightarrow Mn(OH)_7(g)) \end{array} \qquad (R5)$$

In this scheme, sequential water additions to M═O bonds in the studied systems are included, so that finally $M(OH)_x$ is formed, where x is the oxidation state on M. Formation of intermediary water complexes is also included.

2. Methods

Density functional theory was chosen as the method of use for the calculations in this article. A detailed analysis of the performance of DFT and in particular the B3LYP hybrid functional was undertaken for the ScO_2 systems.[6] In order to illustrate the usefulness of this method for transition metal chemistry, also many other Sc_xO_y species were investigated, and results were compared to experiment.[7] A consistent understanding of bonding and stabilities for these oxides emerged from this investigation. Oxyhydroxide and hydroxide formation by water addition to oxides, similar to the reactions of the present work, was studied for the p-element Ge.[8] It becomes interesting to compare the results for Ge to those obtained here for transition metals, especially for the electronical analogue Ti. A detailed presentation on DFT in general and B3LYP in particular was given in the preceding paper,[5] and the internally consistent results in this paper are also good indicators on the performance of this method for transition metal oxides. The application of B3LYP to transition states in the present work is assumed to be valid, as these saddle points are situated between minimum structures with the same stoichiometry, and do not model bond dissociation for which DFT becomes unreliable.

3. Computational Details

The transition metal oxides, oxyhydroxides, and hydroxides in R1−R5 were studied by employing the B3LYP hybrid density functional. The structures were optimized and analytical Hessians evaluated using the GAUSSIAN program package.[9] Thus, information on both energies and vibrational spectra of the systems was obtained. The 6-311G(d) basis sets was used for Sc, Ti, V, Cr, and Mn together with the small 6-311G basis sets (denoted by (S)) for O and H atoms. The larger 6-311+G(2df,2pd) basis sets (L) were used for the first reaction steps, where this was affordable, in order to get higher accuracy and to check the applicability of (S). All calculations were carried out on closed-shell singlet systems, i.e., the ground states of the investigated species, in their highest oxidation state.

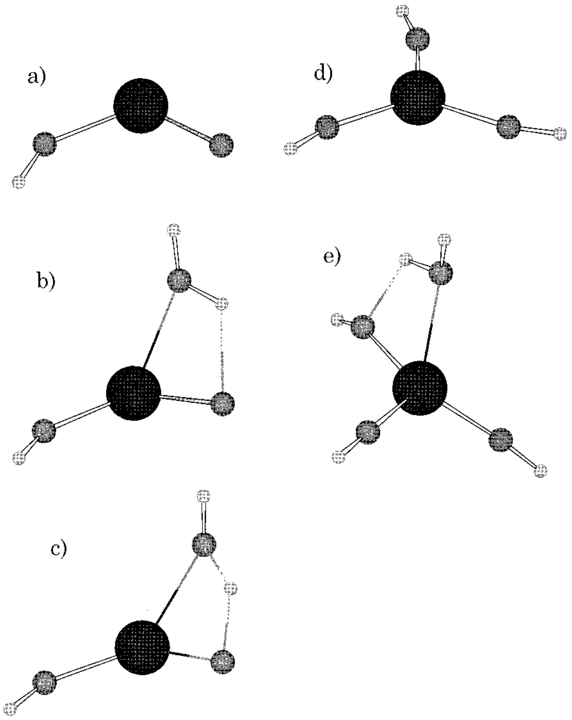

Figure 1. Structures on the potential energy surface of ScO(OH)(g) + $2H_2O(g)$: (a) ScO(OH)(g) (C_s), (b) $ScO(OH){\cdot}H_2O(g)$ (C_1), (c) $ScO(OH){\cdot}H_2O(g)$ (TS) (C_1), (d) $Sc(OH)_3(g)$ (C_{3h}), (e) $Sc(OH)_3{\cdot}H_2O(g)$ (C_1).

4. Results and Discussion

Summaries of structural parameters and vibrational frequencies, together with the corresponding IR intensities, are given in Tables 1−5. Illustrations of relevant structures are found in Figures 1 (Sc), 3 (Ti), 5 (V), 7 (Cr), and 9 (Mn), and of the reaction energetics in Figures 2 (Sc), 4 (Ti), 6 (V), 8 (Cr), and 10 (Mn). All enthalpies, presented there and in the text, are given without inclusion of temperature effects, i.e., at 0 K.

4.1. ScO(OH)(g) + $2H_2O$. O═Sc−OH(g) (Figure 1a) is the simplest neutral oxyhydroxide species of Sc(III). It is also a good starting point for discussing water addition, as it can be understood to form in a model reaction, where water is added to an M−O−M bridge, i.e., O═Sc−O−Sc═O for Sc.[5] The molecule also exemplifies how a symmetry broken solution for ScO_2, which is discussed in detail in ref 6, is stabilized by changing the radical O atom to a hydroxyl group. The ScO(OH) molecule has a planar, bent geometry and C_s symmetry.

Reaction between the O−H bond from water and the Sc═O bond takes place in a plane occupied by these four atoms. Formation of the intermediary $ScO(OH){\cdot}H_2O(g)$ complex (Figure 1b) is exothermic by 98 kJ/mol (L), and it is expected to form without any barrier. The main features of this complex

---

(6) Johnson, J. R. T.; Snis, A.; Panas, I.; Roos, B. O. In preparation.

(7) Johnson, J. R. T.; Panas, I. *Chem. Phys.* **1999**, *248*, 161.

(8) Johnson, J. R. T.; Panas, I. *Chem. Phys.* **1999**, *249*, 273.

(9) Frisch, M. J.; Trucks, G. W.; Schlegel, H. B.; Gill, P. M. W.; Johnson, B. G.; Robb, M. A.; Cheeseman, J. R.; Keith, T.; Petersson, G. A.; Montgomery, J. A.; Raghavachari, K.; Al-Laham, M. A.; Zakrzewski, V. G.; Ortiz, J. V.; Foresman, J. B.; Peng, C. Y.; Ayala, P. Y.; Chen, W.; Wong, M. W.; Andres, J. L.; Replogle, E. S.; Gomperts, R.; Martin, R. L.; Fox, D. J.; Binkley, J. S.; Defrees, D. J.; Baker, J.; Stewart, J. P.; Head-Gordon, M.; Gonzalez, C.; Pople, J. A. *Gaussian 94,* Revision B.3; Gaussian, Inc.: Pittsburgh, PA, 1995.

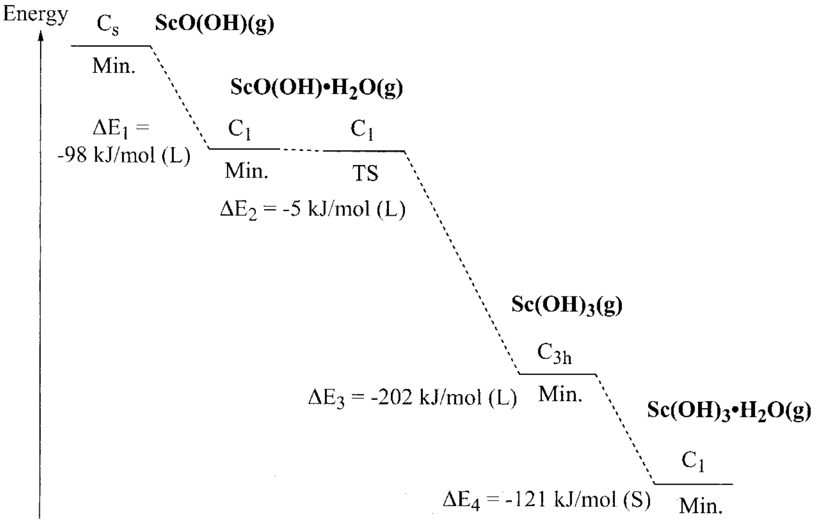

Figure 2. Energetics of reaction 1: ScO(OH)(g) + 2H$_2$O(g).

Table 1. Summaries of Bond Lengths R (Å) and Bond Angles A (deg), and Ranges of Vibrational Frequencies (cm^{-1}), Together with Normal Mode Symmetries and the Number of Vibrations in Each Group, for the ScO(OH) + 2H$_2$O System

		ScO(OH)	
C_s	R(Sc═O): 1.688	R(O−H): 0.958	A(O═Sc−O): 123.4
(L)	R(Sc−O): 1.926		A(Sc−O−H): 145.5
	A′ + A″ (4+1 vib): 173−958	A′ (1 vib): 3935	
		ScO(OH)·H$_2$O	
C_1	R(Sc═O): 1.725	R(O−H): 0.955−0.996	A(O═Sc−O): 125.5
(L)	R(Sc−O): 1.928	R(O···H): 1.924	A(O═Sc···O): 80.1
	R(Sc···O): 2.263	A(Sc−O−H): 148.1	A(O−Sc···O): 132.4
		A(H−O−H): 109.9	A(Sc···O−H): 76.3−136.3
	A (11 vib): 45−910	A (2 vib): 1557−3249	
	A (2 vib): 3876−3941		
		ScO(OH)·H$_2$O (TS)	
C_1	R(Sc═O): 1.763	A(Sc═O···H): 77.3	A(O═Sc−O): 126.7
(L)	R(Sc−O): 1.911	A(Sc−O−H): 152.1	A(O═Sc···O): 74.4
	R(Sc···O): 2.168	A(Sc···O···H): 66.0	A(O−Sc···O): 140.1
	R(O−H): 0.955−0.958	A(Sc···O−H): 139.2	A(O···H···O): 142.2
	R(O···H): 1.131−1.401	A(H−O···H): 113.6	
	A (1 vib): 869i	A (10 vib): 63−902	
	A (2 vib): 1269−1946	A (2 vib): 3899−3946	
		Sc(OH)$_3$	
C_{3h}	R(Sc−O): 1.864	A(O−Sc−O): 120.0	
(S)	R(O−H): 0.959	A(Sc−O−H): 179.0	
	A′ + A″ + E′ + E″ (2+2+3+1 vib): 84−773	A′ + E′ (1+1 vib): 3889	
C_{3h}	R(Sc−O): 1.884	A(O−Sc−O): 120.0	
(L)	R(O−H): 0.954	A(Sc−O−H): 163.5	
	A′ + A″ + E′ + E″ (2+2+3+1 vib): 91−725	A′ + E′ (1+1 vib): 3968−3970	
		Sc(OH)$_3$·H$_2$O	
C_1	R(Sc−O): 1.864−1.959	A(Sc−O−H): 151.7−174.8	A(O−Sc−O): 117.1−117.3
(S)	R(Sc···O): 2.192	A(Sc−O···H): 77.6	A(O−Sc···O): 73.2−115.9
	R(O−H): 0.959−0.997	A(Sc···O−H): 86.8−143.0	A(O−H···O): 122.4
	R(O···H): 1.800	A(H−O−H): 117.3	
	A (18 vib): 69−837	A (2 vib): 154−3248	
	A (3 vib): 3865−3890		

include a Sc···OH$_2$ complex bond (2.26 Å (L)) and a tendency to hydrogen bonding Sc═O···H−OH (1.92 Å (L)) within the reaction plane. The orientation of the reaction plane relative to the nonreactive OH group removes molecular symmetry. The transition state (TS) (Figure 1c) in the subsequent reaction step resembles the ScO(OH)·H$_2$O complex. This is expected, as the Sc···OH$_2$ bond formation renders the active H atom considerable acidity. The major changes on going from the complex to the TS involve optimizing the structure of the reaction plane for transferring the H atom through bending, in conjunction with some changes of the bond distances. At TS, the H atom that is being transferred still resides closer (1.13 Å (L)) to the O atom in the H$_2$O unit than to that of the Sc═O bond (1.40 Å (L)). The calculated energy barrier is very small, 5 kJ/mol (L) without inclusion of ZPE. When the ZPE is taken into account, the barrier disappears and the "TS" structure is 5 kJ/mol (L) below the complex. The total addition reaction can thus be seen to be barrier-free, with the latter step being exothermic by 202 kJ/mol (L). The net energy release of the water addition to ScO(OH) is 305 kJ/mol (L).

The product hydroxide, Sc(OH)$_3$(g) (Figure 1d), is planar and has C_{3h} symmetry, with rather open Sc−O−H bond angles (179° (S) and 164° (L)). Sc has an unoccupied out-of-plane 3d orbital, not used in the σ-bonding to the hydroxyl groups. This orbital

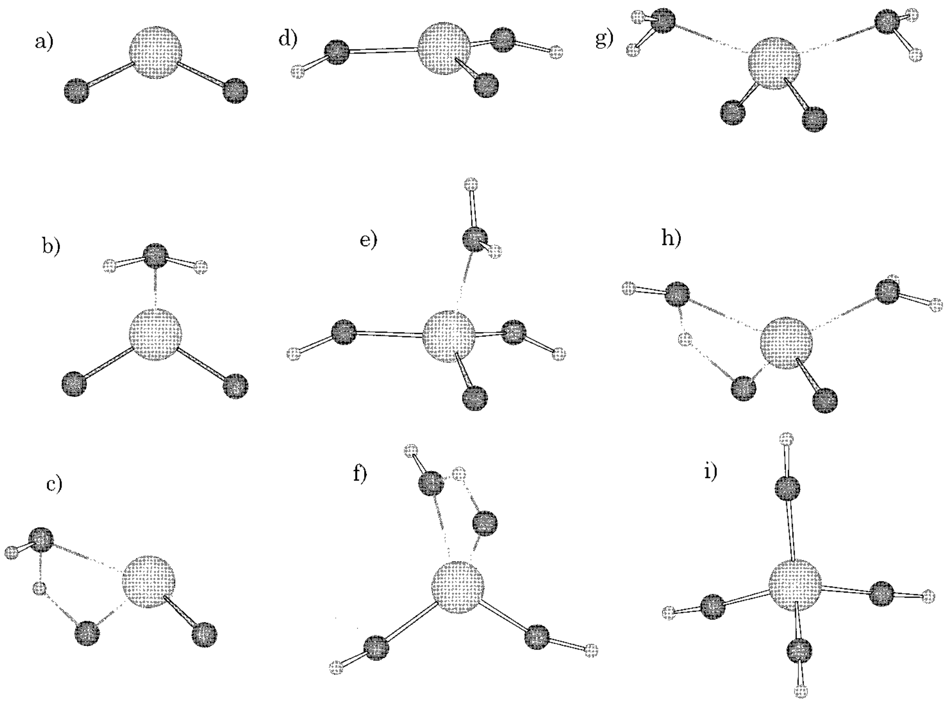

Figure 3. Structures on the potential energy surface of $TiO_2(g) + 2H_2O(g)$: (a) $TiO_2(g)$ (C_{2v}), (b) $TiO_2{\cdot}H_2O(g)$ (C_s), (c) $TiO_2{\cdot}H_2O(g)$ (TS) (C_1), (d) $TiO(OH)_2(g)$ (C_s), (e) $TiO(OH)_2{\cdot}H_2O(g)$ (C_s), (f) $TiO(OH)_2{\cdot}H_2O(g)$ (TS) (C_1), (g) $TiO_2{\cdot}(H_2O)_2(g)$ (C_2), (h) $TiO_2{\cdot}(H_2O)_2(g)$ (TS) (C_1), (i) $Ti(OH)_4(g)$ (C_1).

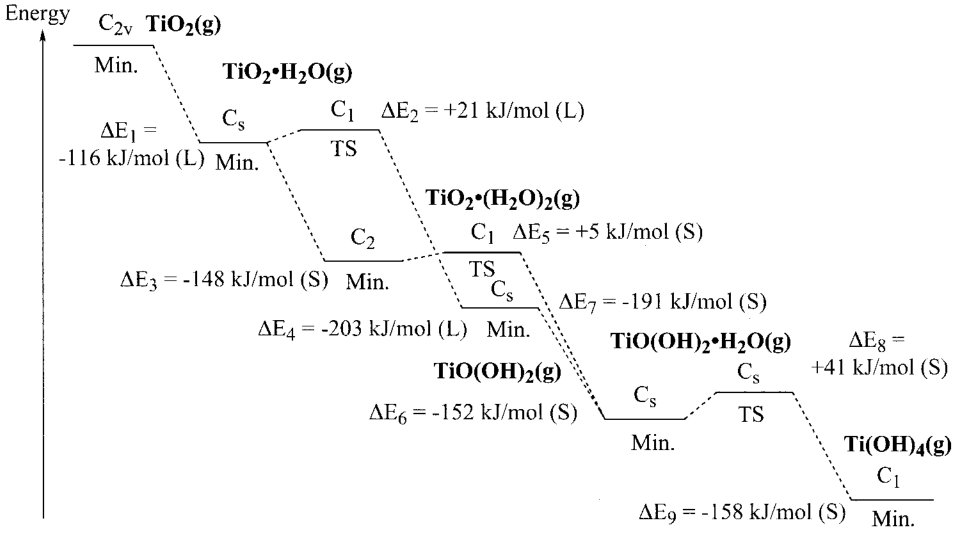

Figure 4. Energetics of reaction 2: $TiO_2(g) + 2H_2O(g)$.

can be used for further complex formation, as it enables a second water molecule to be added to the system and a $Sc(OH)_3{\cdot}H_2O(g)$ complex (Figure 1e) to be formed. Similar to the $ScO(OH){\cdot}H_2O$ complex, this complex has a long $Sc{\cdots}OH_2$ bond (2.19 Å (S)) and a hydrogen bond (1.80 Å (S)). Water addition to $Sc(OH)_3(g)$ is exothermic by 121 kJ/mol (S), and there are no symmetry elements in the resulting complex.

4.2. $TiO_2(g) + 2H_2O$. $TiO_2(g)$ (Figure 3a) is a bent molecule of C_{2v} symmetry with two Ti═O bonds, and two water molecules can be added to these bonds. Although TiO is the simpler oxide, Ti(IV) is more relevant to employ for modeling reactions in an oxidative environment. Also, it represents the most stable oxidation state of Ti in the gas phase, as well as in the bulk. The calculated vibrational frequencies for $TiO_2(g)$ are in agreement with those determined by matrix isolation techniques.[10]

Water reacts with $TiO_2(g)$ perpendicular to the molecular plane to form a stable $TiO_2{\cdot}H_2O(g)$ complex (Figure 3b). Formation of the complex is exothermic by 158 kJ/mol (S) and 116 kJ/mol (L). The poor performance of the smaller basis set for this reaction is mostly due to a poor description of H_2O, as both basis sets produce similar structures. The complex has a slightly pyramidal configuration. The H atoms are directed toward the Ti═O bonds, resulting in C_s symmetry. A $Ti{\cdots}OH_2$ complex bond (2.16 Å (L)) is found, without any hydrogen bonds. Similar to $ScO(OH){\cdot}H_2O(g)$, the subsequent reaction step involves a TS and an energy barrier, while the formation of $TiO_2{\cdot}H_2O(g)$ is barrier-free. The reaction takes place in the plane given by Ti═O and Ti···O−H, which is formed as the mirror plane of the complex is broken. The TS structure (Figure 3c) is

---

[10] Chertihin, G. V.; Andrews, L. *J. Phys. Chem.* **1995**, *99*, 6356.

Table 2. Summaries of Bond Lengths *R* (Å) and Bond Angles *A* (deg), and Ranges of Vibrational Frequencies (cm^{-1}), Together with Normal Mode Symmetries and the Number of Vibrations in Each Group, for the $TiO_2 + 2H_2O$ System

TiO_2			
$C_{\infty v}$	*R*(Ti═O): 1.634	*A*(O═Ti═O):111.5	
(S)	A_1 (1 vib): 377	A_1 + B2 (1+1 vib): 1013−1040	
$C_{\infty v}$	*R*(Ti═O): 1.638	*A*(O═Ti═O) 112.1	
(L)	A_1 (1 vib): 348	A_1 + B2 (1+1 vib): 990−1035	
$TiO_2 \cdot H_2O$			
C_s	*R*(Ti═O):1.651	*R*(O−H): 0.968	*A*(O═Ti═O): 113.4
(S)	*R*(Ti···O): 2.118	*A*(Ti···O−H): 113.2	*A*(O═Ti···O): 99.7
			A(H−O−H): 112.4
A′ + A″ (4+3 vib): 29−577		A′ + A″ (2+1 vib): 998−1669	
A′ + A″ (1+1 vib): 3713−3847			
C_s	*R*(Ti═O):1.654	*R*(O−H): 0.966	*A*(O═Ti═O): 113.7
(L)	*R*(Ti···O): 2.164	*A*(Ti···O−H): 108.5	*A*(O═Ti···O): 102.8
			A(H−O−H): 107.1
A′ + A″ (4+3 vib): 80−564		A′ + A″ (2+1 vib): 973−1635	
A′ + A″ (1+1 vib): 3767−3852			
$TiO_2 \cdot H_2O$ (TS)			
C_1	*R*(Ti═O): 1.628	*R*(O−H): 0.960	*A*(O═Ti−O): 114.5
(L)	*R*(Ti−O): 1.721	*A*(Ti−O···H): 76.1	*A*(O═Ti···O): 125.0
	R(Ti···O): 2.059	*A*(Ti···O−H): 127.3	*A*(O−Ti···O): 77.3
	R(O···H): 1.183−1.341	*A*(Ti···O···H) 65.9	*A*(O···H···O): 132.3
			A(H−O···H): 113.4
A (1 vib): 1358*i*		A (6 vib): 123−922	
A (3 vib): 1035−1887		A (1 vib): 3871	
$TiO(OH)_2$			
C_s	*R*(Ti═O): 1.614	*R*(O−H): 0.961	*A*(O═Ti−O): 115.3
(S)	*R*(Ti−O): 1.809	*A*(Ti−O−H): 151.7	*A*(O−Ti−O): 121.1
A′ + A″ (6+4 vib): 101−1073		A′ + A″ (1+1 vib): 3861−3864	
C_s	*R*(Ti═O): 1.615	*R*(O−H): 0.959	*A*(O═Ti−O): 117.4
(L)	*R*(Ti−O): 1.835		*A*(O−Ti−O): 121.3
A′ + A″ (6+4 vib): 79−1065		A′ + A″ (1+1 vib): 3897−3900	
$TiO_2 \cdot (H_2O)_2$			
C_2	*R*(Ti═O): 1.669	*R*(O−H): 0.965−0.974	*A*(O═Ti═O): 114.4
(S)	*R*(Ti···O): 2.130	*A*(Ti···O−H): 96.2−131.5	*A*(O═Ti···O): 89.6−112.2
		A(H−O−H): 114.1	*A*(O···Ti···O): 140.2
A + B (8+7 vib): 52−984		A + B (1+1 vib): 1612−1616	
A + B (2+2 vib): 3635−3843			
$TiO_2 \cdot (H_2O)_2$ (TS)			
C_1	*R*(Ti═O): 1.637	*A*(Ti−O···H): 77.8	*A*(O═Ti−O): 115.7
(S)	*R*(Ti−O): 1.737	*A*(Ti···O−H): 116.8−144.6	*A*(O═Ti···O): 100.3−129.8
	R(Ti···O): 2.057−2.104	*A*(Ti···O···H): 69.4	*A*(O−Ti···O): 77.0−104.0
	R(O−H): 0.962−0.966	*A*(H−O−H): 113.1	*A*(O···Ti···O): 124.6
	R(O···H): 1.178−1.384	*A*(H−O···H): 122.4	*A*(O···H···O): 135.8
A (1 vib): 1207*i*		A (14 vib): 59−903	
A (4 vib): 1039−1889		A (3 vib): 3730−3867	
$TiO(OH)_2 \cdot H_2O$			
C_s	*R*(Ti═O): 1.634	*A*(Ti−O−H): 146.1	*A*(O═Ti−O): 114.8
(S)	*R*(Ti−O): 1.823	*A*(Ti···O−H): 114.1−131.3	*A*(O═Ti···O): 94.7
	R(Ti···O): 2.096	*A*(H−O−H): 114.6	*A*(O−Ti−O): 116.9
	R(O−H): 0.962−0.966		*A*(O−Ti···O): 106.3
A′ + A″ (8+7 vib): 93−811		A′ (2 vib): 1038−1639	
A′ + A″ (4. vib): 3747−3895			
$TiO(OH)_2 \cdot H_2O$ (TS)			
C_s	*R*(Ti−O): 1.713−1.791	*A*(Ti−O−H): 154.3	*A*(O−Ti−O): 114.4−114.8
(S)	*R*(Ti···O): 1.994	*A*(Ti−O···H): 81.0	*A*(O−Ti···O) 76.2−115.6
	R(O−H): 0.959−0.960	*A*(Ti···O−H): 152.0	*A*(O···H···O): 131.0
	R(O···H): 1.223−1.985	*A*(Ti···O···H): 71.7	*A*(H−O···H): 136.2
A′ (1 vib): 1516*i*		A′ + A″ (9+6 vib): 89−831	
A′ + A″ (2+1 vib): 938−1856		A′ + A″ (2+1 vib): 3875−3888	
$Ti(OH)_4$			
C_1	*R*(Ti−O): 1.779	*A*(O−Ti−O): 109.4−109.5	
(S)	*R*(O−H): 0.957	*A*(Ti−O−H): 172.3−177.6	
A (18 vib): 26−831		A (4 vib): 3925−3932	

reactant-like, with the H atom closer to the water unit (1.18 Å (L)) than to the O atom in the Ti═O bond (1.34 Å (L)), which in turn is short (1.72 Å (L)) as compared to the long Ti···OH_2 bond (2.06 Å (L)). The energy barrier is low, though significant (21 kJ/mol (L)). The continued reaction is exothermic by 203 kJ/mol (L), as the hydrolysis releases 183 kJ/mol (S) and 182 kJ/mol (L). The total exothermicity for water addition to TiO_2(g) becomes 341 kJ/mol (S) and 298 kJ/mol (L). It is emphasized that the enthalpy difference between S and L (43 kJ/mol) mainly results from the energetics of the initial complex formation (42 kJ/mol), while for the actual addition reaction both basis sets perform equally well.

The resulting oxyhydroxide $TiO(OH)_2$(g) (Figure 3d) is also the product of water addition to HO−OTi−O−TiO−OH, which in turn models a Ti−O−Ti bridge in a $(TiO_2)_n$ chain.[5] The energy minimum of $TiO(OH)_2$(g) has C_s symmetry, with the three O atoms bent toward the same side and the OH groups directed toward the remaining Ti═O unit. The relevance of this specific symmetry can be questioned, though, as $TiO(OH)_2$(g) has an inversion barrier of only 2 kJ/mol (S).

An alternative to this reactive route is the formation of the $TiO_2 \cdot (H_2O)_2$(g) complex (Figure 3g). In each of the water units of this system, one OH group is directed toward one of the Ti═O bonds, resulting in C_2 symmetry. The Ti···OH_2 complex bonds are still long (2.13 Å (S)), and no distinct hydrogen bonding is seen. The formation of $TiO_2 \cdot (H_2O)_2$(g) from $TiO_2 \cdot H_2O$(g) and water is exothermic by 148 kJ/mol (S), although a similar effect on the enthalpy due to the small basis set, as was seen above, can be expected. The reaction proceeds via a reactant-like TS (Figure 3h), which much resembles the TS for the reaction of $TiO_2 \cdot H_2O$(g) (Figure 3c). The 5 kJ/mol (S) energy barrier for the former reaction is even lower than that of the latter, although this could be due to basis set effects. The forward reaction is exothermic by 191 kJ/mol (S); thus total energy release in the hydrolysis along this route is 186 kJ/mol (S).

Both this path and the addition of a second water molecule to $TiO(OH)_2$(g) result in the $TiO(OH)_2 \cdot H_2O$(g) complex (Figure 3e) of C_s symmetry. The latter reaction is exothermic by 152 kJ/mol (S). The water molecule approaches $TiO(OH)_2$(g) in the molecular mirror plane, forming a long Ti···OH_2 bond (2.10 Å (S)) and bending somewhat toward the remaining Ti═O bond. The mirror plane is preserved in the TS (Figure 3f), with an energy barrier of 41 kJ/mol (S). In the TS, the H atom is situated between the two O atoms (1.22 and 1.30 Å (S)), but the arrangement is still rather reactant-like. The subsequent reaction is exothermic by 158 kJ/mol (S), and thus the total exothermicity in this step is 117 kJ/mol (S). In total, water addition to $TiO(OH)_2$(g), forming $Ti(OH)_4$(g) (Figure 3i), is exothermic by 269 kJ/mol (S). There are four different (nearly linear) Ti−O−H bond angles in the minimum structure of $Ti(OH)_4$(g), and hence the structure has no symmetry elements, but the central TiO_4 unit displays a perfect tetrahedral configuration. It is therefore possible that the structure is better described having S_4 or even T_d symmetry. The latter point group is expected to apply strictly if all protons are removed.

Table 3. Summaries of Bond Lengths *R* (Å) and Bond Angles *A* (deg), and Ranges of Vibrational Frequencies (cm^{-1}), Together with Normal Mode Symmetries and the Number of Vibrations in Each Group, for the $VO_2(OH) + 2H_2O$ System

		$VO_2(OH)$	
C_1	*R*(V=O): 1.589−1.590	*R*(O−H): 0.960	*A*(O=V=O): 110.3
(S)	*R*(V−O): 1.759	*A*(V−O−H): 155.7	*A*(O=V−O): 116.2−117.1
A (6 vib): 136−828		A (2 vib): 1083−1086	
A (1 vib): 3887			
C_1	*R*(V=O): 1.589−1.590	*R*(O−H): 0.962	*A*(O=V=O): 112.3
(L)	*R*(V−O): 1.794	*A*(V−O−H): 125.8	*A*(O=V−O): 116.7−118.7
A (6 vib): 159−758		A (2 vib): 1075−1079	
A (1 vib): 3860			
		$VO_2(OH){\cdot}H_2O$	
C_1	*R*(V=O): 1.601−1.603	*A*(V−O−H): 143.8	*A*(O=V=O): 111.6
(S)	*R*(V−O): 1.777	*A*(V···O−H): 120.8−122.7	*A*(O=V−O): 114.8−115.3
	R(V···O): 2.032	*A*(H−O−H): 114.0	*A*(O=V···O): 100.9−102.2
	R(O−H): 0.962−0.965		*A*(O−V···O): 110.2
A (12 vib): 65−803		A (3 vib): 1061−1669	
A (3 vib): 3749−3888			
		$VO_2(OH){\cdot}H_2O$ (TS)	
C_1	*R*(V=O): 1.579	*A*(V−O−H): 142.8	*A*(O=V−O): 112.1−112.2
(S)	*R*(V−O): 1.688−1.751	*A*(V−O···H): 79.6	*A*(O=V···O): 115.6
	R(V···O): 1.942	*A*(V···O−H): 137.8	*A*(O−V−O): 116.3
	R(O−H): 0.962−0.964	*A*(V···O···H): 70.6	*A*(O−V···O): 79.1−117.7
	R(O···H): 1.261−1.293	*A*(H−O···H): 129.9	*A*(O···H···O): 130.6
A (1 vib): 1683*i*		A (11 vib): 140−828	
A (4 vib): 942−1821		A (2 vib): 3826−3841	
		$VO(OH)_3$	
C_{3v}	*R*(V=O): 1.575	*R*(O−H): 0.965	*A*(O=V−O): 108.7
(S)	*R*(V−O): 1.757	*A*(V−O−H): 137.3	*A*(O−V−O): 110.3
A_1 + E (4+5 vib): 242−1110		A_1 + E (2+1 vib): 3806−3813	
C_{3v}	*R*(V=O): 1.569	*R*(O−H): 0.962	*A*(O=V−O): 109.4
(L)	*R*(V−O): 1.778	*A*(V−O−H): 122.5	*A*(O−V−O): 109.6
A_1 + E (4+5 vib): 235−1115		A_1 + E (2+1 vib): 3859−3866	
		$VO(OH)_3{\cdot}H_2O$	
C_1	*R*(V=O): 1.578	*R*(O···H): 1.863−2.064	*A*(O−V−O): 104.9−112.9
(S)	*R*(V−O): 1.748−1.804	*A*(V−O−H): 116.9−140.2	*A*(O=V−O): 105.1−112.4
	R(O−H): 0.965−0.990	*A*(V−O···H): 91.5	*A*(O−H···O): 133.8−141.6
		A(H−O−H): 111.0	*A*(H−O···H): 101.8−125.9
A (20 vib): 61−930		A (2 vib): 1106−1650	
A (5 vib): 3411−3814			
		$VO(OH)_3{\cdot}H_2O$ (TS)	
C_1	*R*(V−O): 1.711−1.768	*A*(V−O−H): 110.6−168.4	*A*(O−V−O): 101.7−118.4
(S)	*R*(V···O): 2.147	*A*(V−O···H): 92.8	*A*(O−V···O): 70.8−171.8
	R(O−H): 0.961−0.983	*A*(V···O−H): 117.0	*A*(O···H···O): 128.0
	R(O···H): 1.110−1.402	*A*(V···O···H): 68.3	*A*(H−O···H): 123.4
A (1 vib): 900.4*i*		A (20 vib): 84−944	
A (2 vib): 1178−2003		A (4 vib): 3544−3865	
		$V(OH)_5$	
C_1	*R*(V−O): 1.756−1.838	*A*(O−V−O): 81.3−165.8	
(S)	*R*(O−H): 0.968−0.972	*A*(V−O−H): 115.3−132.3	
A (22 vib): 46−903		A (5 vib): 3697−3773	

4.3. $VO_2(OH)(g) + 2H_2O$. Following similar arguments as for Ti, $VO_2(OH)(g)$ (Figure 5a) is the most suitable simple oxide system for investigating water addition to V under humid conditions in an oxidative environment. $VO_2(OH)(g)$ was also employed to model the product resulting from water addition to a V−O−V bridge, i.e., that in $O_2V{-}O{-}VO_2$.[5] The central vanadium forms a distorted tetrahedron together with the ligating oxygen atoms. The OH group is directed toward one of the V=O bonds, and the molecule therefore lacks symmetry elements, and it has two enantiomers.

The water molecule attacks $VO_2(OH)(g)$ from the uncoordinated side of the V atom, with each H atom pointing towardone of the V=O bonds. The preexisting OH group preserves the low symmetry in the $VO_2(OH){\cdot}H_2O(g)$ complex (Figure 5b). The V···OH_2 complex bond is 2.03 Å (S), whereas no hydrogen bonding to the oxygen in V=O is seen. The complex formation is exothermic by 177 kJ/mol (S). Reaction proceeds via a TS (Figure 5c), in which the water unit is tilted from the pseudo mirror plane toward the V=O bond opposite that toward which the old OH group is directed. The H atom to be transferred is 1.26 Å (S) from the water oxygen and 1.29 Å (S) from that of the V=O bond. The energy barrier is 75 kJ/

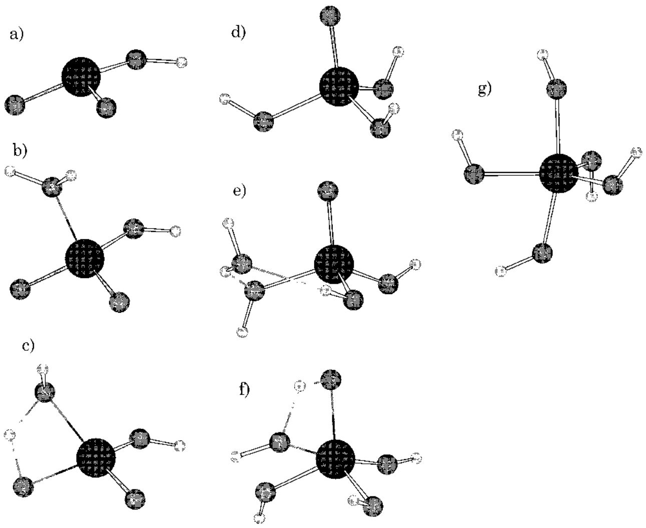

Figure 5. Structures on the potential energy surface of $VO_2(OH)(g) + 2H_2O(g)$: (a) $VO_2(OH)(g)$ (C_1), (b) $VO_2(OH){\cdot}H_2O(g)$ (C_1), (c) $VO_2(OH){\cdot}H_2O(g)$ (TS) (C_1), (d) $VO(OH)_3(g)$ (C_{3v}), (e) $VO(OH)_3{\cdot}H_2O(g)$ (C_1), (f) $VO(OH)_3{\cdot}H_2O(g)$ (TS) (C_1), (g) $V(OH)_5(g)$ (C_1).

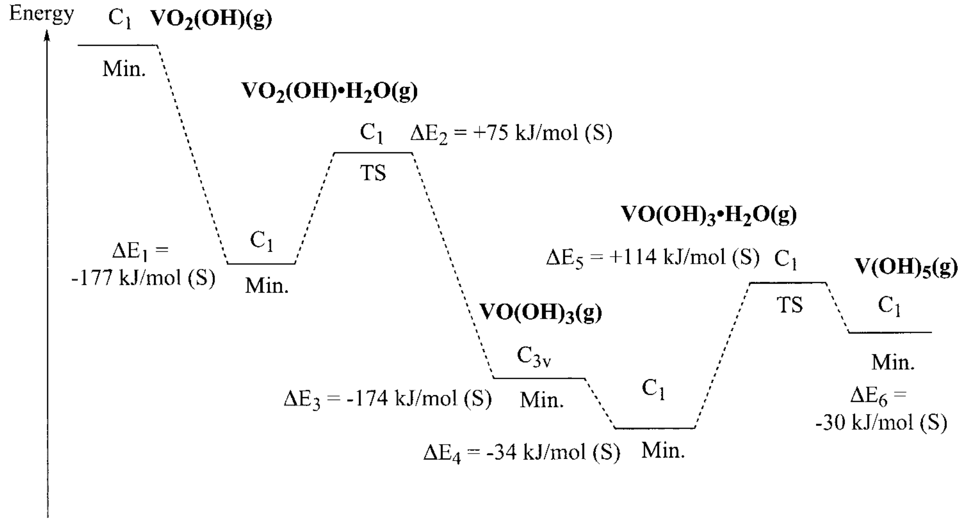

Figure 6. Energetics of reaction 3: $VO_2(OH)(g) + 2H_2O(g)$.

mol (S), and the further reaction is exothermic by 174 kJ/mol (S), which gives a total 99 kJ/mol (S) exothermicity. The total addition process is exothermic by 276 kJ/mol (S) and 233 kJ/mol (L). The discrepancy between the two basis sets (43 kJ/mol) is very similar to that seen for the Ti system (cf. section 4.2), and it is thus also expected to have as common origin the stability of the initial complex.

The oxyhydroxide product is O═V−(OH)$_3$(g) (Figure 5d), where all four O atoms of the central VO_4 unit display a nearly tetrahedral configuration, despite different bond types. The orientation of all three OH groups toward the remaining V═O bond results in C_{3v} symmetry. The V−O−H bond angles are bent significantly (137° (S) and 123° (L)), compared to the nearly linear bond angles in $Ti(OH)_4$(g), telling of the more covalent bonding in $VO(OH)_3$(g).

Addition of a second water molecule to the remaining V═O bond is possible, but the tetrahedral surrounding of the V atom eliminates the possibility to form any initial complex in which an H_2O lone pair is bound directly to V. Instead, the water molecule uses two hydrogen bonds to form the $VO(OH)_3\cdot H_2O$(g) complex (Figure 5e). Although the H atom not used for bonding is oriented toward the V═O bond, the exothermicity for this complex formation (34 kJ/mol (S)) is significantly smaller than what previously was seen for metal-bound water units. The corresponding TS (Figure 5f) is product-like, in that the H atom is closer to the oxygen of the V═O unit (1.11 Å (S)) than to that of the water molecule (1.40 Å (S)). An understanding based on proton transfer implies a significant structural change in the initial step for the H_2O lone pair to bind to the metal ion. The configuration of the O atoms around V also resembles the trigonal bipyramid of the product better than the reactant tetrahedron, and the reaction barrier is high (114 kJ/mol (S)). Despite that 30 kJ/mol (S) is released in the following product formation, the total reaction from the complex is found endothermic by 84 kJ/mol (S).

The structure of the resulting $V(OH)_5$(g) (Figure 5g) displays five inequivalent OH groups, and the V−O bond distances range from 1.76 to 1.84 Å (S). Although this conformation has no symmetry elements, the coordination of O atoms in the central VO_5 unit is rather close to the expected trigonal bipyramid. The reason why this symmetric solution is avoided in the hydroxide is found in the V−O σ-bonds, which put additional constraints on the molecular orbitals, as compared to a pure oxide. The V−O−H bond angles are similar to those in $VO(OH)_3$(g), ranging from 115° to 132° (S), due to O···H intramolecular interactions on the verge of hydrogen bonding. The total endothermicity for adding the second water (50 kJ/mol (S)) reflects the problematic bonding in $V(OH)_5$(g). Rather, the more favorable arrangement of surrounding water molecules in a moist atmosphere would be to produce solvated $VO(OH)_3$(aq).

4.4. CrO_3(g) + $3H_2O$. CrO_3(g) is a possible product of a disintegrating protective chromium oxide scale.[5] This species has a transition state in D_{3h} symmetry, for which a slight bending results in a stable C_{3v} structure (Figure 7a). The energy is lowered by 22 kJ/mol (S) and 13 kJ/mol (L) due to the increase in Cr═O bonding achieved by employing the out-of-plane Cr 3d orbitals. The resulting CrO_3(g) structure is open on one side, which makes the molecule accessible for bonding to an incoming nucleophile, such as water. The IR-active vibrational frequencies for CrO_3(g), obtained from matrix isolation experiments,[11] fit with the calculated frequencies.

Water addition to CrO_3(g) results in an initial $CrO_3\cdot H_2O$(g) complex (Figure 7b) of C_s symmetry. The complex resembles the reacting species, with a long Cr···OH_2 bond (1.98 Å), but no hydrogen bonds. The complex formation is exothermic by 205 kJ/mol (S) and 146 kJ/mol (L) and is achieved without any energy barrier. Again, a decreased exothermicity is seen for the primary complex forming reaction step when using (L). The reaction, though, has a high barrier (108 kJ/mol (S)) to the following TS (Figure 7c). The reaction takes place in the plane formed by the reactive OH group in the water unit and the Cr═O bond in the molecular mirror plane. The bending of the unreactive OH group out of this plane removes all molecular symmetry. The H to be transferred is situated between the water oxygen (1.29 Å (S)) and that of Cr═O (1.28 Å (S)). The Cr−O bond distances (1.90 and 1.69 Å (S)) are accordingly halfway between the reactant and product values. The continued reaction is exothermic by 175 kJ/mol (S), resulting in a net exothermicity of 67 kJ/mol (S) and 87 kJ/mol (L) for the hydrolysis step.

The product $CrO_2(OH)_2$(g) molecule (Figure 7d) has a second-order saddle point in C_{2v} symmetry, with symmetry-breaking vibrations of A_2 and B_1 symmetries. These vibrations correspond to the two choices available for rotating the H atoms in order to maximize electrostatic attraction to the Cr═O bonds

---

(11) Chertihin, G. V.; Bare W. D.; Andrews, L. *J. Chem. Phys.* **1997**, *107*, 2798.

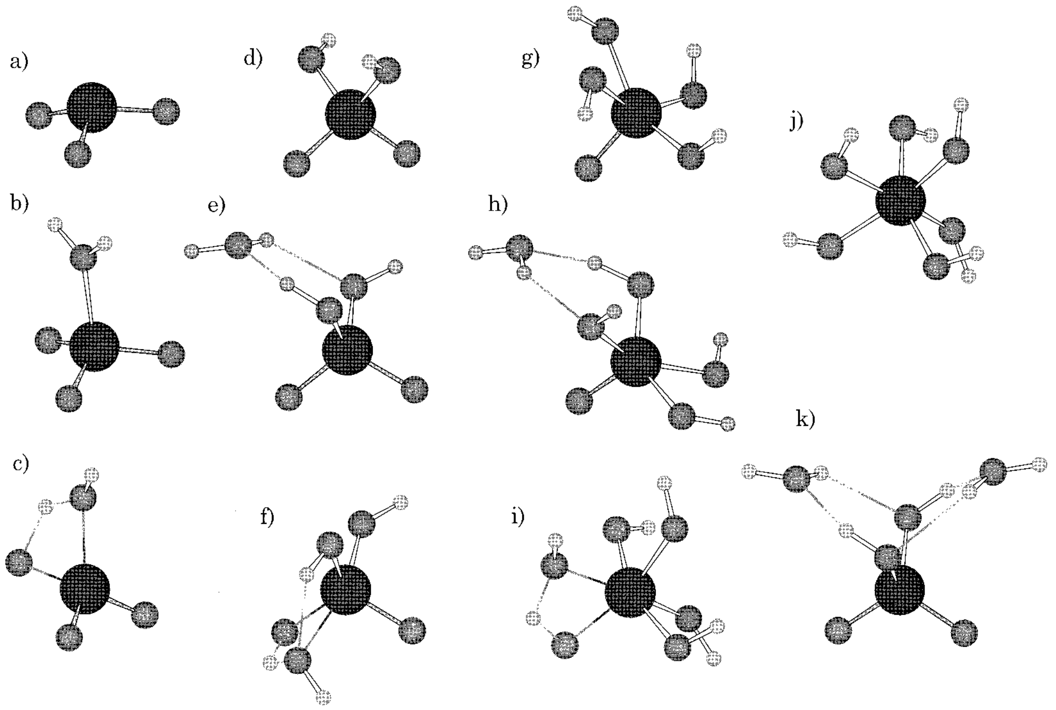

Figure 7. Structures on the potential energy surface of $CrO_3(g) + 3H_2O(g)$: (a) $CrO_3(g)$ (C_{3v}), (b) $CrO_3{\cdot}H_2O(g)$ (C_s), (c) $CrO_3{\cdot}H_2O(g)$ (TS) (C_1), (d) $CrO_2(OH)_2(g)$ (C_2), (e) $CrO_2(OH)_2{\cdot}H_2O(g)$ (C_1), (f) $CrO_2(OH)_2{\cdot}H_2O(g)$ (TS) (C_1), (g) $CrO(OH)_4(g)$ (C_1), (h) $CrO(OH)_4{\cdot}H_2O(g)$ (C_1), (i) $CrO(OH)_4{\cdot}H_2O(g)$ (TS) (C_1), (j) $Cr(OH)_6(g)$ (C_1), (k) $CrO_2(OH)_2{\cdot}(H_2O)_2(g)$.

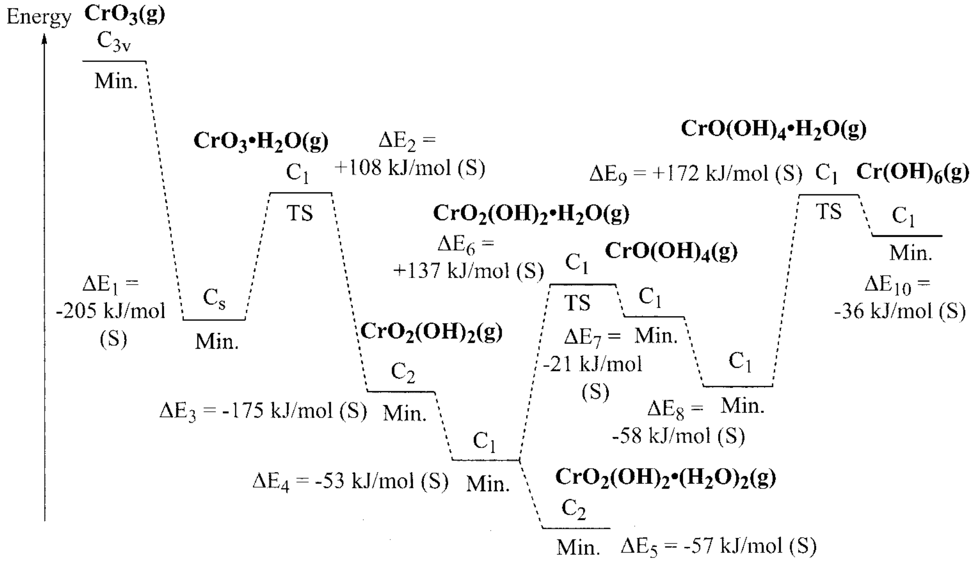

Figure 8. Energetics of reaction 4: $CrO_3(g) + 3H_2O(g)$.

and lead to C_s and C_2 minima, respectively, of which the latter is the most stable structure. The rotational barriers are small, 3 kJ/mol (S) and 7 kJ/mol (S) for each of the symmetries, respectively. The barriers are somewhat increased (14 kJ/mol (L) and 17 kJ/mol (L)) when the basis set is increased. For the C_2 structure there are also two enantiomers, where the Cr−OH groups are directed either clockwise or counterclockwise. The total affinity for water addition to $CrO_3(g)$ to form $CrO_2(OH)_2(g)$ is 272 kJ/mol (S) and 233 kJ/mol (L). This difference (39 kJ/mol) resembles that found for the vanadium system (cf. section 4.3), while it can be seen here that an error in the complex formation exothermicity is somewhat compensated for in the additive step.

The remaining two Cr═O bonds can successively react with water. Similar to $VO(OH)_3{\cdot}H_2O(g)$, the initial complex has no $Cr{\cdots}OH_2$ bond. Instead, two hydrogen bonds are used to bind water. These *two* bonds fix the arrangement of the Cr−OH groups to that of the C_2 structure of $CrO_2(OH)_2(g)$, although the complex has no symmetry elements. The formation of the $CrO_2(OH)_2{\cdot}H_2O(g)$ complex (Figure 7e) is exothermic by 53 kJ/mol (S). In similarity to $CrO_2(OH)_2(g)$, there are two enantiomers for the water complex. The TS of the addition reaction (Figure 7f) is product-like, with the transferring H closer to the accepting O (1.10 Å (S)) than that of the water unit (1.42 Å (S)). While the O from water has approached its product position by moving a significant distance, the $Cr{\cdots}OH_2$ bond is still long (2.18 Å (S)). These structural considerations are reflected in the large energy barrier for reaction (137 kJ/mol (S)), and in that only 21 kJ/mol (S) is released on product formation. Thus the total reaction step is endothermic by 116

Table 4. Summaries of Bond Lengths R (Å) and Bond Angles A (deg), and Ranges of Vibrational Frequencies (cm^{-1}), Together with Normal Mode Symmetries and the Number of Vibrations in Each Group, for the $CrO_3 + 3H_2O$ System

		CrO_3	
D_{3h}	R(Cr═O): 1.577	A(O═Cr═O): 120.0	
(S)	A_2'' (1 vib): 249i	$A_1' + E'$ (1+2 vib): 374−1121	
C_{3v}	R(Cr═O): 1.578	A(O═Cr═O): 113.2	
(S)	$A_1 + E$ (1+1 vib): 302−402	$A_1 + E$ (1+1 vib): 1024−1095	
C_{3v}	R(Cr═O): 1.576	A(O═Cr═O): 114.8	
(L)	$A_1 + E$ (1+1 vib): 244−386	$A_1 + E$ (1+1 vib): 1018−1090	
		$CrO_3 \cdot H_2O$	
C_s	R(Cr═O): 1.584−1.589	R(O−H): 0.965	A(O═Cr═O): 113.1−114.0
(S)	R(Cr···O): 1.978	A(Cr···O−H): 120.9−124.4	A(O═Cr···O): 101.2−106.6
			A(H−O−H): 114.7
$A' + A''$ (5+4 vib): 68−683		$A' + A''$ (3+1 vib): 1017−1675	
A' (2 vib): 3754−3891			
C_s	R(Cr═O): 1.582−1.587	R(O−H): 0.961	A(O═Cr═O): 113.3−114.1
(L)	R(Cr···O): 2.009	A(Cr···O−H): 122.0−126.5	A(O═Cr···O): 101.1−106.4
			A(H−O−H): 111.5
		$CrO_3 \cdot H_2O$ (TS)	
C_1	R(Cr═O): 1.564−1.569	A(Cr−O···H): 71.5	A(O═Cr═O): 111.0
(S)	R(Cr−O): 1.671	A(Cr···O−H): 133.3	A(O═Cr−O): 115.2−116.1
	R(Cr···O): 1.900	A(Cr···O···H): 80.5	A(O═Cr···O): 112.8−119.0
	R(O−H): 0.964	A(H−O···H): 134.8	A(O−Cr···O): 79.7
	R(O···H) 1.275−1.286		A(O···H···O): 126.2
A (1 vib): 1789i		A (10 vib): 154−960	
A (3 vib): 1091−1798		A (1 vib): 3817	
		$CrO_2(OH)_2$	
C_{2v}	R(Cr═O): 1.567	R(O−H): 0.967	A(O═Cr═O): 107.4
(S)	R(Cr−O): 1.729	A(Cr−O−H): 137.5	A(O═Cr−O): 110.2
			A(O−Cr−O): 108.7
$A_2 + B_1$ (2 vib): 213i−105i		$A_1 + A_2 + B_1 + B_2$ (5+1+2+3 vib): 266−1114	
$A_1 + B_2$ (1+1 vib): 3740−3745			
C_{2v}	R(Cr═O): 1.562	R(O−H): 0.963	A(O═Cr═O): 107.3
(L)	R(Cr−O): 1.749	A(Cr−O−H): 124.3	A(O═Cr−O): 110.4
			A(O−Cr−O): 107.8
$A_2 + B_1$ (2 vib): 309i−239i		$A_1 + A_2 + B_1 + B_2$ (5+1+2+3 vib): 246−1088	
$A_1 + B_2$ (1+1 vib): 3842−3846			
C_s	R(Cr═O) 1.564−1.565	R(O−H): 0.969	A(O═Cr═O): 109.2
(S)	R(Cr−O): 1.738	A(Cr−O−H): 130.0	A(O═Cr−O): 109.0−110.2
			A(O−Cr−O): 109.2
$A' + A''$ (8+5 vib): 205−1112		$A' + A''$ (1+1 vib): 3751−3757	
C_s	R(Cr═O): t1.559−1.561	R(O−H): 0.965	A(O═Cr═O): 111.3
(L)	R(Cr−O): 1.758	A(Cr−O−H): 116.3	A(O═Cr−O): 108.6−110.1
			A(O−Cr−O): 109.2
C_2	R(Cr═O): 1.565	R(O−H): 0.970	A(O═Cr═O): 110.4
(S)	R(Cr−O): 1.739	A(Cr−O−H): 128.5	A(O═Cr−O): 108.4−109.4
			A(O−Cr−O): 110.0
A + B (7+6 vib): 217−1114		A + B (1+1 vib): 3740−3745	
C_2	R(Cr═O): 1.560	R(O−H): 0.965	A(O═Cr═O): 111.3
(L)	R(Cr−O): 1.757	A(Cr−O−H): 115.8	A(O═Cr−O): 107.8−109.9
			A(O−Cr−O): 110.0
		$CrO_2(OH)_2 \cdot H_2O$	
C_1	R(Cr═O): 1.562−1.569	A(Cr−O−H): 111.3−125.8	A(O═Cr═O): 111.0
(S)	R(Cr−O): 1.724−1.772	A(Cr−O···H): 93.3	A(O═Cr−O): 107.3−111.7
	R(O−H): 0.966−0.978	A(H−O−H): 112.2	A(O−Cr−O): 106.4
	R(O···H): 1.760−2.080	A(H−O···H): 107.0−130.7	A(O−H···O): 132.8−138.9
A (19 vib): 67−1129		A (2 vib): 1640−3246	
A (3 vib): 3593−3821			
		$CrO_2(OH)_2 \cdot H_2O$ (TS)	
C_1	R(Cr═O): 1.560	A(Cr−O−H): 108.7−137.6	A(O═Cr−O): 106.5−112.0
(S)	R(Cr−O): 1.696−1.740	A(Cr−O···H): 95.7	A(O═Cr···O): 89.5
	R(Cr···O): 2.181	A(Cr···O−H): 118.9	A(O−Cr−O): 99.3−122.3
	R(O−H): 0.968−0.990	A(Cr···O···H): 67.0−68.0	A(O−Cr···O): 69.8−163.9
	R(O···H): 1.100−1.419−1.887		A(O···H···O): 109.4−126.4
		A(H−O···H): 120.4−120.6	A(H···O···H): 115.9
A (1 vib): 831i		A (19 vib): 137−1149	
A (2 vib): 2069−3429		A (2 vib): 3701−3768	
		$CrO(OH)_4$	
C_1	R(Cr═O):1.551	R(O−H): 0.973−0.978	A(O═Cr−O): 103.9−109.1
(S)	R(Cr−O): 1.757−1.860	A(Cr−O−H): 108.8−125.8	A(O−Cr−O): 76.2−145.8
A (20 vib): 94−1118		A (4 vib): 3610−3699	
		$CrO_2(OH)_2 \cdot (H_2O)_2$	
C_2	R(Cr═O): 1.566	A(Cr−O−H): 111.3	A(O═Cr═O): 111.6
(S)	R(Cr−O): 1.753	A(Cr−O···H): 93.6	A(O═Cr−O): 108.3
	R(O−H): 0.966−1.001	A(H−O−H): 112.6	A(O−Cr−O): 102.9
	R(O···H): 1.730−2.122	A(H−O···H): 128.5−135.2	A(O−H···O): 107.3−140.9
A + B (13+12 vib): 43−1147		A + B (2+2 vib): 1635−3235	
A + B (2+2 vib): 3590−3828			
		$CrO(OH)_4 \cdot H_2O$	
C_1	R(Cr═O): 1.555	A(Cr−O−H): 110.0−121.3	A(O═Cr−O): 101.2−109.4
(S)	R(Cr−O): 1.767−1.859	A(Cr−O···H): 103.1	A(O−Cr−O): 77.1−150.0
	R(O−H): 0.966−1.012	A(H−O−H): 113.2	A(O−H···O): 136.5−151.2
	R(O···H): 1.651−1.908	A(H−O···H): 98.9−130.5	
A (26 vib): 69−1197		A (2 vib): 1618−3001	
A (5 vib): 3510−3820			
		$CrO(OH)_4 \cdot H_2O$ (TS)	
C_1	R(Cr−O): 1.691−1.995	A(Cr−O−H): 112.4−144.6	A(O−Cr−O): 70.4−169.7
(S)	R(O−H): 0.967−0.979	A(Cr−O···H): 76.5−91.8	A(O−H···O): 120.9
	R(O···H): 1.192−1.268	A(H−O···H): 144.6	
A (1 vib): 1485i		A (26 vib): 125−1075	
A (1 vib): 1886		A (5 vib): 3621−3773	
		$Cr(OH)_6$	
C_1	R(Cr−O): 1.757−1.867	A(Cr−O−H): 110.5−115.3	A(O−Cr−O): 77.7−166.6
(S)	R(O−H): 0.974−0.980		
A (27 vib): 144−1006		A (6 vib): 3593−3672	

kJ/mol (S), whereas water addition to $CrO_2(OH)_2$(g) becomes endothermic by 63 kJ/mol (S).

The product of this second water addition is O═Cr−$(OH)_4$(g) (Figure 7g), where the energy minimum has no symmetry elements, although the configuration on the central CrO_5 unit closely resembles a square-based pyramid. As was seen for $V(OH)_5$(g) (cf. section 4.3), the distortion from high symmetry (C_{4v}) and the endothermicity for formation of $CrO(OH)_4$(g) both

Table 5. Summaries of Bond Lengths *R* (Å) and Bond Angles *A* (deg), and Ranges of Vibrational Frequencies (cm^{-1}), Together with Normal Mode Symmetries and the Number of Vibrations in Each Group, for the $MnO_3(OH) + H_2O$ System

		$MnO_3(OH)$	
C_s	*R*(Mn=O): 1.563−1.566	*R*(O−H): 0.974	*A*(O=Mn=O): 109.6−111.2
(S)	*R*(Mn−O): 1.733	*A*(Mn−O−H): 122.9	*A*(O=Mn−O): 106.6−109.0
	A′ + A″ (7+4 vib): 208−1079	A′ (1 vib): 3680	
		$MnO_3(OH)\cdot H_2O$	
C_1	*R*(Mn=O): 1.566−1.575	*A*(Mn−O−H): 117.2	*A*(O=Mn=O): 109.5−111.5
(S)	*R*(Mn−O): 1.708	*A*(H−O−H): 112.7	*A*(O=Mn−O): 107.4−109.4
	R(O−H): 0.965−1.013	*A*(H−O···H): 118.5−128.7	*A*(O−H···O): 163.5
	R(O···H): 1.572		
	A (16 vib): 16−1068	A (3 vib): 1213−2982	
	A (2 vib): 3719−3875		
		$MnO_3(OH)\cdot H_2O$ (TS)	
C_1	*R*(Mn=O): 1.560−1.572	*A*(Mn−O−H): 117.3	*A*(O=Mn=O): 112.1
(S)	*R*(Mn−O): 1.708−1.755	*A*(Mn−O···H): 89.6	*A*(O=Mn−O): 102.7−124.2
	R(Mn···O): 2.069	*A*(Mn···O−H): 121.7	*A*(O=Mn···O): 84.0−89.7
	R(O−H): 0.973−0.976	*A*(Mn···O···H): 73.0	*A*(O−Mn−O): 89.6
	R(O···H): 1.204−1.256	*A*(H−O···H): 127.9	*A*(O−Mn···O): 70.5−158.9
			A(O···H···O): 126.7
	A (1 vib): 1595*i*	A (16 vib): 86−1054	
	A (2 vib): 1193−1840	A (2 vib): 3663−3697	
		$MnO_2(OH)_3$	
C_1	*R*(Mn=O): 1.552−1.575	*R*(O−H): 0.977−0.981	*A*(O=Mn=O): 110.4
(S)	*R*(Mn−O): 1.767−1.900	*A*(Mn−O−H): 108.2−113.3	
		A(O=Mn−O): 85.0−136.7	*A*(O−Mn−O): 76.0−149.8
	A (18 vib): 100−1111	A (3 vib): 3568−3636	

reflect the problem to optimize the Cr−OH bonding in this pentacoordinated configuration. It is, though, interesting to note that the remaining Cr=O bond results in a different framework structure for this molecule than for the V system. The initial $CrO(OH)_4\cdot H_2O$(g) complex (Figure 7h) of the third water addition is similar to that of the second reaction, in that the water unit is bonded by two hydrogen bonds. The complex formation is exothermic by 58 kJ/mol (S). Again, the addition reaction has a product-like TS (Figure 7i), with a quite short $Cr\cdots OH_2$ bond (2.00 Å (S)). The transferring H is still, though, between the accepting O (1.19 Å (S)) and the water unit (1.27 Å (S)), whereas the two O atoms are closer to each other than in the previous TS structure (vide supra). The energy barrier for the reactants is 172 kJ/mol (S), while product formation releases 36 kJ/mol (S). This reaction step is thereby endothermic by 136 kJ/mol (S), and the total reaction from $CrO(OH)_4$(g) by 78 kJ/mol.

The final product of the water additions is the hydroxide $Cr(OH)_6$(g) (Figure 7j). In this structure, the OH groups form a distorted octahedron. This distortion is clearly seen in that the Cr−O bond distances are distributed in a range from 1.76 to 1.87 Å (S), which is similar to what was found for $V(OH)_5$(g). The OH groups are close to forming intramolecular hydrogen bonds and display highly bent Cr−O−H bond angles (111°−115° (S)). Condensation of all the Cr−OH groups in $Cr(OH)_6$(g) is expected to produce a bulk chromium oxide with octahedral coordination on Cr, with a structure similar to that of WO_3(s).[12] However, the actual structure of CrO_3(s) is that of polymeric chains consisting of tetrahedrally coordinated Cr, and in fact this coordination is the only observed one for Cr(VI) in bulk or solution, due to the fact that this ion is smaller than W(VI).[12] Indeed, the preference of tetrahedral coordination for Cr(VI) is reflected in the instability of $Cr(OH)_6$(g), as compared to $CrO_2(OH)_2$(g) + $2H_2O$.

Following this understanding, an alternative to the additive scheme is to use hydrogen bonding for attaching a second water molecule to $CrO_2(OH)_2\cdot H_2O$(g). The product is the $CrO_2(OH)_2\cdot(H_2O)_2$(g) complex (Figure 7k), which preserves the C_2 symmetry of $CrO_2(OH)_2$(g). This reaction is exothermic by 57 kJ/mol (S), and $CrO_2(OH)_2\cdot(H_2O)_2$(g) is therefore concluded to be the most stable species in the CrO_3(g) + $3H_2O$ system. The either clockwise or counterclockwise orientation of the two Cr−OH groups results in two eneantiomers for $CrO_2(OH)_2\cdot(H_2O)_2$(g), as for $CrO_2(OH)_2$(g). As was seen for the transition states of the two paths in the TiO_2(g) + $2H_2O$ system (cf. section 4.2), it seems plausible to assume that the TS leading from $CrO_2(OH)_2\cdot(H_2O)_2$(g) to $CrO(OH)_4\cdot H_2O$(g) is similar to that from $CrO_2(OH)_2\cdot H_2O$(g) to $CrO(OH)_4$(g). In conjunction with this TS, a similar large energy barrier (∼137 kJ/mol (S)) is expected. The reverse reaction is expected display a small barrier (∼21 kJ/mol (S)), which will destabilize the former species on behalf of the latter.

The high affinity toward water addition makes CrO_3(g) an unstable species under humid conditions at low temperatures. Such an instability of CrO_3(g) is in agreement with thermodynamical estimates[13] and with a recent quantum chemical study by Espelid et al.[14] Their results for CrO_3(g) and $CrO_2(OH)_2$(g) are in agreement with those obtained here. It is, though, expected that in an excess of water $CrO_2(OH)_2$(g) will undergo further reactions to form hydrogen-bonded water complexes, similar to $CrO_2(OH)_2\cdot H_2O$(g) and $CrO_2(OH)_2\cdot(H_2O)_2$(g), as the energy barrier toward further addition to the remaining Cr=O bonds limits the importance of these species (vide supra). Thus, the final product under moist conditions will be the solvated chromic acid, H_2CrO_4(aq).

4.5. $MnO_3(OH)$(g) + $3H_2O$. $MnO_3(OH)$(g) (Figure 9a) is the simplest, neutral singlet oxyhydroxide for Mn(VII), and it can also be seen as the resulting product of water addition to Mn_2O_7(g).[5] The positioning of the OH group between two of the Mn=O units gives the minimum C_s symmetry. As the central MnO_4 unit already displays a nearly tetrahedral configuration, water addition takes place by initially forming a complex using hydrogen bonding to the OH group. The formation of the MnO3-

---

(12) Greenwood, N. N.; Earnshaw, A. *Chemistry of the Elements*, 2nd ed.; Butterworth-Heinemann: Oxford, 1997.

(13) Ebbinghaus, B. B. *Combust. Flame* **1995**, *101*, 311.

(14) Espelid, Ø.; Børve, K. J.; Jensen, V. R. *J. Phys. Chem. A* **1998**, *102*, 10414.

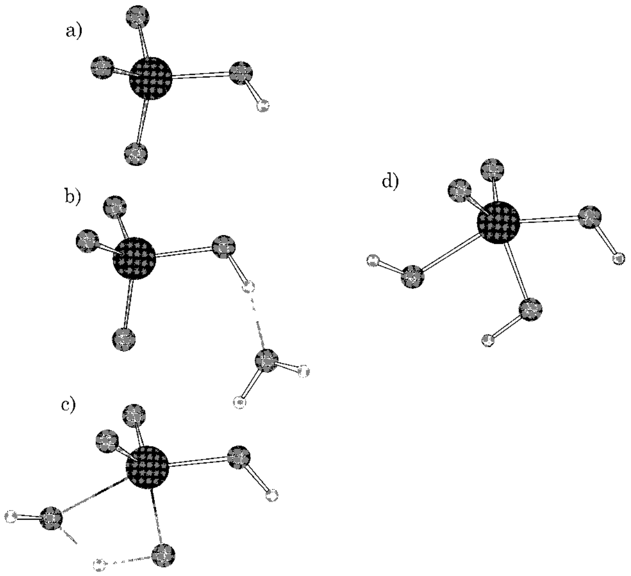

Figure 9. Structures on the potential energy surface of $MnO_3(OH)(g) + H_2O(g)$: (a) $MnO_3(OH)(g)$ (C_s), (b) $MnO_3(OH)\cdot H_2O(g)$ (C_1), (c) $MnO_3(OH)\cdot H_2O(g)$ (TS) (C_1), (d) $MnO_2(OH)_3(g)$ (C_1).

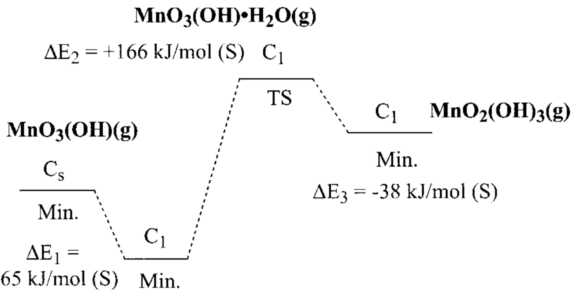

Figure 10. Energetics of reaction 5: $MnO_3(OH)(g) + H_2O(g)$.

$(OH)\cdot H_2O(g)$ complex (Figure 9b) is exothermic by 65 kJ/mol (S). The single connecting hydrogen bond makes the water unit floppy in its positioning relative to the M═O bonds, and the energy minimum has no symmetry elements. The TS structure (Figure 9c) for the addition is product-like, and the incoming water approaches Mn on the side opposite the Mn−OH group with an Mn···OH_2 bond length of 2.10 Å (S). It could, though, be argued that the water complex corresponding to the TS has the water unit on this side of the metal ion. However, no such water complex was found. The energy barrier from the reactants is large (166 kJ/mol (S)), while only 38 kJ/mol (S) is released when the product is formed. Thus, the addition step is endothermic by 128 kJ/mol (S), and the total process from $MnO_3(OH)(g)$ by 65 kJ/mol (S).

The trigonal bipyramid structure of $MnO_2(OH)_3(g)$ (Figure 9d) is even more distorted than that of $V(OH)_5(g)$. Again, this distortion originates from the strained Mn−OH bonds, which are in a range from 1.77 to 1.90 Å (S). Although water addition to the remaining two Mn═O bonds is possible, $MnO(OH)_5(g)$ was found to collapse into a peroxide structure, and the addition process still very endothermic. It therefore seems likely that neither $MnO(OH)_5(g)$ nor $Mn(OH)_7(g)$ is a stable compound, thus making the continued addition uninteresting. The reason for this structural collapse probably is the severe difficulties in combining the Mn valence orbitals to form five Mn−OH σ bonds, in conjunction with Mn═O bonding in $MnO(OH)_5(g)$. The product of $MnO_3(OH)(g)$ and water in a moist atmosphere is, though, expected to be the solvated $MnO_3(OH)(aq)$.

5. Conclusions

Reaction with water is a common route for chemically induced deterioration of protective oxide scales on metals. Two possible scenarios for the role of water can be thought of: one in which H_2O is permanently consumed as $MO_x(OH)_y$ species desorb and a second where water acts as a catalyst, being liberated from the hydroxide species in the gas phase, thereby forming molecular or cluster oxides. The present investigation mainly concerned the former class of reactions, while the latter processes were considered in the preceding paper.[5]

A general understanding of water addition to transition metal oxides and oxyhydroxides emerges from the comparative computational study on systems in the series Sc, Ti, V, Cr, and Mn. Water addition is exothermic if the metal center has fewer than four ligands coordinated. The reaction begins by forming a stable water complex with an M···OH_2 bond. This first step is exothermic and barrier-free. In the second reaction step, addition takes place as an H is transferred from the water unit to an M═O bond, and subsequently two M-OH groups are formed. This step in the addition process is associated with a transition state and an energy barrier.

When the system has achieved a tetrahedral structure, it is still possible to add water as long as M═O bonds remain. These reactions are, however, endothermic, while the formation of hydrogen-bonded water complexes is exothermic. The latter processes result in solvation of the tetrahedrally coordinated oxyhydroxide kernels, as there are no M···OH_2 bonds in these complexes. For the investigated transition metal species, the sequence of such kernels was found to be $Sc(OH)_3\cdot H_2O(g)$, $Ti(OH)_4(g)$, $VO(OH)_3(g)$, $CrO_2(OH)_2(g)$, and $MnO_3(OH)(g)$.

The result is important for understanding the stability of $CrO_2(OH)_2(g)$, the product of water addition to the model $CrO_3(s)$ chains.[5] Although the most stable species in the $CrO_3(g) + 3H_2O$ system is the $CrO_2(OH)_2\cdot(H_2O)_2(g)$ complex, it is found that the attachment of water only stabilizes the symmetry and structure of the core molecule. This supports a local mechanism for water-induced decomposition of chromium oxide, in which $CrO_2(OH)_2(g)$ is produced, and points to product solvation as a decisive effect for the deterioration of oxide scales.

Acknowledgment. This work was supported by the Swedish Natural Sciences Research Council.

Supporting Information Available: Tables listing detailed structural parameters, absolute energies, and vibrational frequencies. This material is available free of charge via the Internet at http://pubs.acs.org.

IC991150H